

Measurement of the Time-Dependent CP Asymmetry in $B^0 \rightarrow D_{CP}^{(*)}h^0$ Decays

B. Aubert,¹ M. Bona,¹ D. Boutigny,¹ Y. Karyotakis,¹ J. P. Lees,¹ V. Poireau,¹ X. Prudent,¹ V. Tisserand,¹
A. Zghiche,¹ J. Garra Tico,² E. Grauges,² L. Lopez,³ A. Palano,³ G. Eigen,⁴ I. Ofte,⁴ B. Stugu,⁴ L. Sun,⁴
G. S. Abrams,⁵ M. Battaglia,⁵ D. N. Brown,⁵ J. Button-Shafer,⁵ R. N. Cahn,⁵ Y. Groysman,⁵ R. G. Jacobsen,⁵
J. A. Kadyk,⁵ L. T. Kerth,⁵ Yu. G. Kolomensky,⁵ G. Kukartsev,⁵ D. Lopes Pegna,⁵ G. Lynch,⁵ L. M. Mir,⁵
T. J. Orimoto,⁵ M. Pripstein,⁵ N. A. Roe,⁵ M. T. Ronan,⁵ * K. Tackmann,⁵ W. A. Wenzel,⁵ P. del Amo Sanchez,⁶
C. M. Hawkes,⁶ A. T. Watson,⁶ T. Held,⁷ H. Koch,⁷ B. Lewandowski,⁷ M. Pelizaeus,⁷ T. Schroeder,⁷ M. Steinke,⁷
J. T. Boyd,⁸ J. P. Burke,⁸ W. N. Cottingham,⁸ D. Walker,⁸ D. J. Asgeirsson,⁹ T. Cuhadar-Donszelmann,⁹
B. G. Fulsom,⁹ C. Hearty,⁹ N. S. Knecht,⁹ T. S. Mattison,⁹ J. A. McKenna,⁹ A. Khan,¹⁰ M. Saleem,¹⁰
L. Teodorescu,¹⁰ V. E. Blinov,¹¹ A. D. Bukin,¹¹ V. P. Druzhinin,¹¹ V. B. Golubev,¹¹ A. P. Onuchin,¹¹
S. I. Serednyakov,¹¹ Yu. I. Skovpen,¹¹ E. P. Solodov,¹¹ K. Yu Todyshev,¹¹ M. Bondioli,¹² M. Bruinsma,¹² S. Curry,¹²
I. Eschrich,¹² D. Kirkby,¹² A. J. Lankford,¹² P. Lund,¹² M. Mandelkern,¹² E. C. Martin,¹² D. P. Stoker,¹²
S. Abachi,¹³ C. Buchanan,¹³ S. D. Foulkes,¹⁴ J. W. Gary,¹⁴ F. Liu,¹⁴ O. Long,¹⁴ B. C. Shen,¹⁴ L. Zhang,¹⁴
H. P. Paar,¹⁵ S. Rahatlou,¹⁵ V. Sharma,¹⁵ J. W. Berryhill,¹⁶ C. Campagnari,¹⁶ A. Cunha,¹⁶ B. Dahmes,¹⁶
T. M. Hong,¹⁶ D. Kovalskiy,¹⁶ J. D. Richman,¹⁶ T. W. Beck,¹⁷ A. M. Eisner,¹⁷ C. J. Flacco,¹⁷ C. A. Heusch,¹⁷
J. Kroseberg,¹⁷ W. S. Lockman,¹⁷ T. Schalk,¹⁷ B. A. Schumm,¹⁷ A. Seiden,¹⁷ D. C. Williams,¹⁷ M. G. Wilson,¹⁷
L. O. Winstrom,¹⁷ E. Chen,¹⁸ C. H. Cheng,¹⁸ A. Dvoretzki,¹⁸ F. Fang,¹⁸ D. G. Hitlin,¹⁸ I. Narsky,¹⁸ T. Piatenko,¹⁸
F. C. Porter,¹⁸ G. Mancinelli,¹⁹ B. T. Meadows,¹⁹ K. Mishra,¹⁹ M. D. Sokoloff,¹⁹ F. Blanc,²⁰ P. C. Bloom,²⁰
S. Chen,²⁰ W. T. Ford,²⁰ J. F. Hirschauer,²⁰ A. Kreisel,²⁰ M. Nagel,²⁰ U. Nauenberg,²⁰ A. Olivas,²⁰ J. G. Smith,²⁰
K. A. Ulmer,²⁰ S. R. Wagner,²⁰ J. Zhang,²⁰ A. Chen,²¹ E. A. Eckhart,²¹ A. Soffer,²¹ W. H. Toki,²¹ R. J. Wilson,²¹
F. Winklmeier,²¹ Q. Zeng,²¹ D. D. Altenburg,²² E. Feltresi,²² A. Hauke,²² H. Jasper,²² J. Merkel,²² A. Petzold,²²
B. Spaan,²² K. Wacker,²² T. Brandt,²³ V. Klose,²³ H. M. Lacker,²³ W. F. Mader,²³ R. Nogowski,²³ J. Schubert,²³
K. R. Schubert,²³ R. Schwierz,²³ J. E. Sundermann,²³ A. Volk,²³ D. Bernard,²⁴ G. R. Bonneaud,²⁴ E. Latour,²⁴
Ch. Thiebaux,²⁴ M. Verderi,²⁴ P. J. Clark,²⁵ W. Gradl,²⁵ F. Muheim,²⁵ S. Playfer,²⁵ A. I. Robertson,²⁵ Y. Xie,²⁵
M. Andreotti,²⁶ D. Bettoni,²⁶ C. Bozzi,²⁶ R. Calabrese,²⁶ A. Cecchi,²⁶ G. Cibinetto,²⁶ P. Franchini,²⁶ E. Luppi,²⁶
M. Negri,²⁶ A. Petrella,²⁶ L. Piemontese,²⁶ E. Prencipe,²⁶ V. Santoro,²⁶ F. Anulli,²⁷ R. Baldini-Ferrolì,²⁷
A. Calcaterra,²⁷ R. de Sangro,²⁷ G. Finocchiaro,²⁷ S. Pacetti,²⁷ P. Patteri,²⁷ I. M. Peruzzi,²⁷ † M. Piccolo,²⁷
M. Rama,²⁷ A. Zallo,²⁷ A. Buzzo,²⁸ R. Contri,²⁸ M. Lo Vetere,²⁸ M. M. Macri,²⁸ M. R. Monge,²⁸ S. Passaggio,²⁸
C. Patrignani,²⁸ E. Robutti,²⁸ A. Santroni,²⁸ S. Tosi,²⁸ K. S. Chaisanguanthum,²⁹ M. Morii,²⁹ J. Wu,²⁹
R. S. Dubitzky,³⁰ J. Marks,³⁰ S. Schenk,³⁰ U. Uwer,³⁰ D. J. Bard,³¹ P. D. Dauncey,³¹ R. L. Flack,³¹ J. A. Nash,³¹
M. B. Nikolich,³¹ W. Panduro Vazquez,³¹ P. K. Behera,³² X. Chai,³² M. J. Charles,³² U. Mallik,³² N. T. Meyer,³²
V. Ziegler,³² J. Cochran,³³ H. B. Crawley,³³ L. Dong,³³ V. Eyges,³³ W. T. Meyer,³³ S. Prell,³³ E. I. Rosenberg,³³
A. E. Rubin,³³ A. V. Gritsan,³⁴ C. K. Lae,³⁴ A. G. Denig,³⁵ M. Fritsch,³⁵ G. Schott,³⁵ N. Arnaud,³⁶
J. Béguilleux,³⁶ M. Davier,³⁶ G. Grosdidier,³⁶ A. Höcker,³⁶ V. Lepeltier,³⁶ F. Le Diberder,³⁶ A. M. Lutz,³⁶
S. Pruvot,³⁶ S. Rodier,³⁶ P. Roudeau,³⁶ M. H. Schune,³⁶ J. Serrano,³⁶ V. Sordini,³⁶ A. Stocchi,³⁶ W. F. Wang,³⁶
G. Wormser,³⁶ D. J. Lange,³⁷ D. M. Wright,³⁷ C. A. Chavez,³⁸ I. J. Forster,³⁸ J. R. Fry,³⁸ E. Gabathuler,³⁸
R. Gamet,³⁸ D. E. Hutchcroft,³⁸ D. J. Payne,³⁸ K. C. Schofield,³⁸ C. Touramanis,³⁸ A. J. Bevan,³⁹ K. A. George,³⁹
F. Di Lodovico,³⁹ W. Menges,³⁹ R. Sacco,³⁹ G. Cowan,⁴⁰ H. U. Flaecher,⁴⁰ D. A. Hopkins,⁴⁰ P. S. Jackson,⁴⁰
T. R. McMahon,⁴⁰ F. Salvatore,⁴⁰ A. C. Wren,⁴⁰ D. N. Brown,⁴¹ C. L. Davis,⁴¹ J. Allison,⁴² N. R. Barlow,⁴²
R. J. Barlow,⁴² Y. M. Chia,⁴² C. L. Edgar,⁴² G. D. Lafferty,⁴² T. J. West,⁴² J. I. Yi,⁴² J. Anderson,⁴³ C. Chen,⁴³
A. Jawahery,⁴³ D. A. Roberts,⁴³ G. Simi,⁴³ J. M. Tuggle,⁴³ G. Blaylock,⁴⁴ C. Dallapiccola,⁴⁴ S. S. Hertzbach,⁴⁴
X. Li,⁴⁴ T. B. Moore,⁴⁴ E. Salvati,⁴⁴ S. Saremi,⁴⁴ R. Cowan,⁴⁵ P. H. Fisher,⁴⁵ G. Sciolla,⁴⁵ S. J. Sekula,⁴⁵
M. Spitznagel,⁴⁵ F. Taylor,⁴⁵ R. K. Yamamoto,⁴⁵ H. Kim,⁴⁶ S. E. Mclachlin,⁴⁶ P. M. Patel,⁴⁶ S. H. Robertson,⁴⁶
A. Lazzaro,⁴⁷ V. Lombardo,⁴⁷ F. Palombo,⁴⁷ J. M. Bauer,⁴⁸ L. Cremaldi,⁴⁸ V. Eschenburg,⁴⁸ R. Godang,⁴⁸
R. Kroeger,⁴⁸ D. A. Sanders,⁴⁸ D. J. Summers,⁴⁸ H. W. Zhao,⁴⁸ S. Brunet,⁴⁹ D. Côté,⁴⁹ M. Simard,⁴⁹ P. Taras,⁴⁹
F. B. Viaud,⁴⁹ H. Nicholson,⁵⁰ G. De Nardo,⁵¹ F. Fabozzi,⁵¹ ‡ L. Lista,⁵¹ D. Monorchio,⁵¹ C. Sciacca,⁵¹
M. A. Baak,⁵² G. Raven,⁵² H. L. Snoek,⁵² C. P. Jessop,⁵³ J. M. LoSecco,⁵³ G. Benelli,⁵⁴ L. A. Corwin,⁵⁴

K. K. Gan,⁵⁴ K. Honscheid,⁵⁴ D. Hufnagel,⁵⁴ H. Kagan,⁵⁴ R. Kass,⁵⁴ J. P. Morris,⁵⁴ A. M. Rahimi,⁵⁴ J. J. Regensburger,⁵⁴ R. Ter-Antonyan,⁵⁴ Q. K. Wong,⁵⁴ N. L. Blount,⁵⁵ J. Brau,⁵⁵ R. Frey,⁵⁵ O. Igonkina,⁵⁵ J. A. Kolb,⁵⁵ M. Lu,⁵⁵ R. Rahmat,⁵⁵ N. B. Sinev,⁵⁵ D. Strom,⁵⁵ J. Strube,⁵⁵ E. Torrence,⁵⁵ N. Gagliardi,⁵⁶ A. Gaz,⁵⁶ M. Margoni,⁵⁶ M. Morandin,⁵⁶ A. Pompili,⁵⁶ M. Posocco,⁵⁶ M. Rotondo,⁵⁶ F. Simonetto,⁵⁶ R. Stroili,⁵⁶ C. Voci,⁵⁶ E. Ben-Haim,⁵⁷ H. Briand,⁵⁷ J. Chauveau,⁵⁷ P. David,⁵⁷ L. Del Buono,⁵⁷ Ch. de la Vaissière,⁵⁷ O. Hamon,⁵⁷ B. L. Hartfiel,⁵⁷ Ph. Leruste,⁵⁷ J. Malclès,⁵⁷ J. Ocariz,⁵⁷ A. Perez,⁵⁷ L. Gladney,⁵⁸ M. Biasini,⁵⁹ R. Covarelli,⁵⁹ E. Manoni,⁵⁹ C. Angelini,⁶⁰ G. Batignani,⁶⁰ S. Bettarini,⁶⁰ G. Calderini,⁶⁰ M. Carpinelli,⁶⁰ R. Cenci,⁶⁰ F. Forti,⁶⁰ M. A. Giorgi,⁶⁰ A. Lusiani,⁶⁰ G. Marchiori,⁶⁰ M. A. Mazur,⁶⁰ M. Morganti,⁶⁰ N. Neri,⁶⁰ E. Paoloni,⁶⁰ G. Rizzo,⁶⁰ J. J. Walsh,⁶⁰ M. Haire,⁶¹ J. Biesiada,⁶² P. Elmer,⁶² Y. P. Lau,⁶² C. Lu,⁶² J. Olsen,⁶² A. J. S. Smith,⁶² A. V. Telnov,⁶² E. Baracchini,⁶³ F. Bellini,⁶³ G. Cavoto,⁶³ A. D'Orazio,⁶³ D. del Re,⁶³ E. Di Marco,⁶³ R. Faccini,⁶³ F. Ferrarotto,⁶³ F. Ferroni,⁶³ M. Gaspero,⁶³ P. D. Jackson,⁶³ L. Li Gioi,⁶³ M. A. Mazzoni,⁶³ S. Morganti,⁶³ G. Piredda,⁶³ F. Polci,⁶³ F. Renga,⁶³ C. Voena,⁶³ M. Ebert,⁶⁴ H. Schröder,⁶⁴ R. Waldi,⁶⁴ T. Adye,⁶⁵ G. Castelli,⁶⁵ B. Franek,⁶⁵ E. O. Olaiya,⁶⁵ S. Ricciardi,⁶⁵ W. Roethel,⁶⁵ F. F. Wilson,⁶⁵ R. Aleksan,⁶⁶ S. Emery,⁶⁶ M. Escalier,⁶⁶ A. Gaidot,⁶⁶ S. F. Ganzhur,⁶⁶ G. Hamel de Monchenault,⁶⁶ W. Kozanecki,⁶⁶ M. Legendre,⁶⁶ G. Vasseur,⁶⁶ Ch. Yèche,⁶⁶ M. Zito,⁶⁶ X. R. Chen,⁶⁷ H. Liu,⁶⁷ W. Park,⁶⁷ M. V. Purohit,⁶⁷ J. R. Wilson,⁶⁷ M. T. Allen,⁶⁸ D. Aston,⁶⁸ R. Bartoldus,⁶⁸ P. Bechtle,⁶⁸ N. Berger,⁶⁸ R. Claus,⁶⁸ J. P. Coleman,⁶⁸ M. R. Convery,⁶⁸ J. C. Dingfelder,⁶⁸ J. Dorfan,⁶⁸ G. P. Dubois-Felsmann,⁶⁸ D. Dujmic,⁶⁸ W. Dunwoodie,⁶⁸ R. C. Field,⁶⁸ T. Glanzman,⁶⁸ S. J. Gowdy,⁶⁸ M. T. Graham,⁶⁸ P. Grenier,⁶⁸ V. Halyo,⁶⁸ C. Hast,⁶⁸ T. Hryn'ova,⁶⁸ W. R. Innes,⁶⁸ M. H. Kelsey,⁶⁸ P. Kim,⁶⁸ D. W. G. S. Leith,⁶⁸ S. Li,⁶⁸ S. Luitz,⁶⁸ V. Luth,⁶⁸ H. L. Lynch,⁶⁸ D. B. MacFarlane,⁶⁸ H. Marsiske,⁶⁸ R. Messner,⁶⁸ D. R. Muller,⁶⁸ C. P. O'Grady,⁶⁸ V. E. Ozcan,⁶⁸ A. Perazzo,⁶⁸ M. Perl,⁶⁸ T. Pulliam,⁶⁸ B. N. Ratcliff,⁶⁸ A. Roodman,⁶⁸ A. A. Salnikov,⁶⁸ R. H. Schindler,⁶⁸ J. Schwiening,⁶⁸ A. Snyder,⁶⁸ J. Stelzer,⁶⁸ D. Su,⁶⁸ M. K. Sullivan,⁶⁸ K. Suzuki,⁶⁸ S. K. Swain,⁶⁸ J. M. Thompson,⁶⁸ J. Va'vra,⁶⁸ N. van Bakel,⁶⁸ A. P. Wagner,⁶⁸ M. Weaver,⁶⁸ W. J. Wisniewski,⁶⁸ M. Wittgen,⁶⁸ D. H. Wright,⁶⁸ A. K. Yarritu,⁶⁸ K. Yi,⁶⁸ C. C. Young,⁶⁸ P. R. Burchat,⁶⁹ A. J. Edwards,⁶⁹ S. A. Majewski,⁶⁹ B. A. Petersen,⁶⁹ L. Wilden,⁶⁹ S. Ahmed,⁷⁰ M. S. Alam,⁷⁰ R. Bula,⁷⁰ J. A. Ernst,⁷⁰ V. Jain,⁷⁰ B. Pan,⁷⁰ M. A. Saeed,⁷⁰ F. R. Wappler,⁷⁰ S. B. Zain,⁷⁰ W. Bugg,⁷¹ M. Krishnamurthy,⁷¹ S. M. Spanier,⁷¹ R. Eckmann,⁷² J. L. Ritchie,⁷² A. M. Ruland,⁷² C. J. Schilling,⁷² R. F. Schwitters,⁷² J. M. Izen,⁷³ X. C. Lou,⁷³ S. Ye,⁷³ F. Bianchi,⁷⁴ F. Gallo,⁷⁴ D. Gamba,⁷⁴ M. Pelliccioni,⁷⁴ M. Bomben,⁷⁵ L. Bosisio,⁷⁵ C. Cartaro,⁷⁵ F. Cossutti,⁷⁵ G. Della Ricca,⁷⁵ L. Lanceri,⁷⁵ L. Vitale,⁷⁵ V. Azzolini,⁷⁶ N. Lopez-March,⁷⁶ F. Martinez-Vidal,⁷⁶ D. A. Milanese,⁷⁶ A. Oyanguren,⁷⁶ J. Albert,⁷⁷ Sw. Banerjee,⁷⁷ B. Bhuyan,⁷⁷ K. Hamano,⁷⁷ R. Kowalewski,⁷⁷ I. M. Nugent,⁷⁷ J. M. Roney,⁷⁷ R. J. Sobie,⁷⁷ J. J. Back,⁷⁸ P. F. Harrison,⁷⁸ T. E. Latham,⁷⁸ G. B. Mohanty,⁷⁸ M. Pappagallo,^{78,§} H. R. Band,⁷⁹ X. Chen,⁷⁹ S. Dasu,⁷⁹ K. T. Flood,⁷⁹ J. J. Hollar,⁷⁹ P. E. Kutter,⁷⁹ Y. Pan,⁷⁹ M. Pierini,⁷⁹ R. Prepost,⁷⁹ S. L. Wu,⁷⁹ Z. Yu,⁷⁹ and H. Neal⁸⁰

(The BABAR Collaboration)

¹Laboratoire de Physique des Particules, IN2P3/CNRS et Université de Savoie, F-74941 Annecy-Le-Vieux, France

²Universitat de Barcelona, Facultat de Física, Departament ECM, E-08028 Barcelona, Spain

³Università di Bari, Dipartimento di Fisica and INFN, I-70126 Bari, Italy

⁴University of Bergen, Institute of Physics, N-5007 Bergen, Norway

⁵Lawrence Berkeley National Laboratory and University of California, Berkeley, California 94720, USA

⁶University of Birmingham, Birmingham, B15 2TT, United Kingdom

⁷Ruhr Universität Bochum, Institut für Experimentalphysik 1, D-44780 Bochum, Germany

⁸University of Bristol, Bristol BS8 1TL, United Kingdom

⁹University of British Columbia, Vancouver, British Columbia, Canada V6T 1Z1

¹⁰Brunel University, Uxbridge, Middlesex UB8 3PH, United Kingdom

¹¹Budker Institute of Nuclear Physics, Novosibirsk 630090, Russia

¹²University of California at Irvine, Irvine, California 92697, USA

¹³University of California at Los Angeles, Los Angeles, California 90024, USA

¹⁴University of California at Riverside, Riverside, California 92521, USA

¹⁵University of California at San Diego, La Jolla, California 92093, USA

¹⁶University of California at Santa Barbara, Santa Barbara, California 93106, USA

¹⁷University of California at Santa Cruz, Institute for Particle Physics, Santa Cruz, California 95064, USA

¹⁸California Institute of Technology, Pasadena, California 91125, USA

¹⁹University of Cincinnati, Cincinnati, Ohio 45221, USA

²⁰University of Colorado, Boulder, Colorado 80309, USA

²¹Colorado State University, Fort Collins, Colorado 80523, USA

²²Universität Dortmund, Institut für Physik, D-44221 Dortmund, Germany

- ²³Technische Universität Dresden, Institut für Kern- und Teilchenphysik, D-01062 Dresden, Germany
- ²⁴Laboratoire Leprince-Ringuet, CNRS/IN2P3, Ecole Polytechnique, F-91128 Palaiseau, France
- ²⁵University of Edinburgh, Edinburgh EH9 3JZ, United Kingdom
- ²⁶Università di Ferrara, Dipartimento di Fisica and INFN, I-44100 Ferrara, Italy
- ²⁷Laboratori Nazionali di Frascati dell'INFN, I-00044 Frascati, Italy
- ²⁸Università di Genova, Dipartimento di Fisica and INFN, I-16146 Genova, Italy
- ²⁹Harvard University, Cambridge, Massachusetts 02138, USA
- ³⁰Universität Heidelberg, Physikalisches Institut, Philosophenweg 12, D-69120 Heidelberg, Germany
- ³¹Imperial College London, London, SW7 2AZ, United Kingdom
- ³²University of Iowa, Iowa City, Iowa 52242, USA
- ³³Iowa State University, Ames, Iowa 50011-3160, USA
- ³⁴Johns Hopkins University, Baltimore, Maryland 21218, USA
- ³⁵Universität Karlsruhe, Institut für Experimentelle Kernphysik, D-76021 Karlsruhe, Germany
- ³⁶Laboratoire de l'Accélérateur Linéaire, IN2P3/CNRS et Université Paris-Sud 11, Centre Scientifique d'Orsay, B. P. 34, F-91898 ORSAY Cedex, France
- ³⁷Lawrence Livermore National Laboratory, Livermore, California 94550, USA
- ³⁸University of Liverpool, Liverpool L69 7ZE, United Kingdom
- ³⁹Queen Mary, University of London, E1 4NS, United Kingdom
- ⁴⁰University of London, Royal Holloway and Bedford New College, Egham, Surrey TW20 0EX, United Kingdom
- ⁴¹University of Louisville, Louisville, Kentucky 40292, USA
- ⁴²University of Manchester, Manchester M13 9PL, United Kingdom
- ⁴³University of Maryland, College Park, Maryland 20742, USA
- ⁴⁴University of Massachusetts, Amherst, Massachusetts 01003, USA
- ⁴⁵Massachusetts Institute of Technology, Laboratory for Nuclear Science, Cambridge, Massachusetts 02139, USA
- ⁴⁶McGill University, Montréal, Québec, Canada H3A 2T8
- ⁴⁷Università di Milano, Dipartimento di Fisica and INFN, I-20133 Milano, Italy
- ⁴⁸University of Mississippi, University, Mississippi 38677, USA
- ⁴⁹Université de Montréal, Physique des Particules, Montréal, Québec, Canada H3C 3J7
- ⁵⁰Mount Holyoke College, South Hadley, Massachusetts 01075, USA
- ⁵¹Università di Napoli Federico II, Dipartimento di Scienze Fisiche and INFN, I-80126, Napoli, Italy
- ⁵²NIKHEF, National Institute for Nuclear Physics and High Energy Physics, NL-1009 DB Amsterdam, The Netherlands
- ⁵³University of Notre Dame, Notre Dame, Indiana 46556, USA
- ⁵⁴Ohio State University, Columbus, Ohio 43210, USA
- ⁵⁵University of Oregon, Eugene, Oregon 97403, USA
- ⁵⁶Università di Padova, Dipartimento di Fisica and INFN, I-35131 Padova, Italy
- ⁵⁷Laboratoire de Physique Nucléaire et de Hautes Energies, IN2P3/CNRS, Université Pierre et Marie Curie-Paris6, Université Denis Diderot-Paris7, F-75252 Paris, France
- ⁵⁸University of Pennsylvania, Philadelphia, Pennsylvania 19104, USA
- ⁵⁹Università di Perugia, Dipartimento di Fisica and INFN, I-06100 Perugia, Italy
- ⁶⁰Università di Pisa, Dipartimento di Fisica, Scuola Normale Superiore and INFN, I-56127 Pisa, Italy
- ⁶¹Prairie View A&M University, Prairie View, Texas 77446, USA
- ⁶²Princeton University, Princeton, New Jersey 08544, USA
- ⁶³Università di Roma La Sapienza, Dipartimento di Fisica and INFN, I-00185 Roma, Italy
- ⁶⁴Universität Rostock, D-18051 Rostock, Germany
- ⁶⁵Rutherford Appleton Laboratory, Chilton, Didcot, Oxon, OX11 0QX, United Kingdom
- ⁶⁶DSM/Dapnia, CEA/Saclay, F-91191 Gif-sur-Yvette, France
- ⁶⁷University of South Carolina, Columbia, South Carolina 29208, USA
- ⁶⁸Stanford Linear Accelerator Center, Stanford, California 94309, USA
- ⁶⁹Stanford University, Stanford, California 94305-4060, USA
- ⁷⁰State University of New York, Albany, New York 12222, USA
- ⁷¹University of Tennessee, Knoxville, Tennessee 37996, USA
- ⁷²University of Texas at Austin, Austin, Texas 78712, USA
- ⁷³University of Texas at Dallas, Richardson, Texas 75083, USA
- ⁷⁴Università di Torino, Dipartimento di Fisica Sperimentale and INFN, I-10125 Torino, Italy
- ⁷⁵Università di Trieste, Dipartimento di Fisica and INFN, I-34127 Trieste, Italy
- ⁷⁶IFIC, Universitat de Valencia-CSIC, E-46071 Valencia, Spain
- ⁷⁷University of Victoria, Victoria, British Columbia, Canada V8W 3P6
- ⁷⁸Department of Physics, University of Warwick, Coventry CV4 7AL, United Kingdom
- ⁷⁹University of Wisconsin, Madison, Wisconsin 53706, USA
- ⁸⁰Yale University, New Haven, Connecticut 06511, USA

(Dated: February 8, 2020)

We report a measurement of the time-dependent CP -asymmetry parameters \mathcal{S} and \mathcal{C} in color-suppressed $B^0 \rightarrow D^{(*)0}h^0$ decays, where h^0 is a π^0 , η , or ω meson, and the D^0 decays to one of the CP eigenstates K^+K^- , $K_s^0\pi^0$, or $K_s^0\omega$. The data sample consists of 383×10^6 $\Upsilon(4S) \rightarrow B\bar{B}$ decays collected with the *BABAR* detector at the PEP-II asymmetric-energy B -factory at SLAC. The results are $\mathcal{S} = -0.56 \pm 0.23 \pm 0.05$ and $\mathcal{C} = -0.23 \pm 0.16 \pm 0.04$, where the first error is statistical and the second is systematic.

PACS numbers: 13.25.Hw, 12.15.Hh, 11.30.Er

Measurements of time-dependent CP asymmetries in B^0 meson decays, through the interference between decays with and without B^0 - \bar{B}^0 mixing, have provided stringent tests on the mechanism of CP violation in the standard model (SM). The time-dependent CP asymmetry amplitude $\sin 2\beta$ has been measured with high precision in the $b \rightarrow c\bar{c}s$ decay modes [1], where $\beta = -\arg(V_{cd}V_{cb}^*/V_{td}V_{tb}^*)$ is a phase in the Cabibbo-Kobayashi-Maskawa (CKM) quark-mixing matrix [2].

In this Letter, we present a measurement of the time-dependent CP asymmetry in B^0 meson decays to a neutral D meson and a light neutral meson through a $b \rightarrow c\bar{u}d$ color-suppressed tree amplitude. Interference between decay amplitudes with and without B^0 - \bar{B}^0 mixing contribution occurs if the neutral D meson decays to a CP eigenstate. The measured time-dependent asymmetry is expected to be different from $\sin 2\beta$ measured in the charmonium modes due to the sub-leading amplitude $b \rightarrow u\bar{c}d$, which has a different weak phase. This amplitude is suppressed by $V_{ub}V_{cd}^*/V_{cb}V_{ud}^* \simeq 0.02$ relative to the leading diagram. Therefore the deviation is expected to be small in the SM [3, 4].

Many other decay modes that have significant contribution from loop diagrams have also been studied [5] to constrain or discover new physics due to unobserved heavy particles in the loop diagrams in B decays. This kind of new physics would not affect the decays presented in this Letter because only tree diagrams contribute to these modes. However, R -parity-violating supersymmetric processes [3] could enter at tree level in these decays, leading to a deviation from the SM prediction.

The analysis uses a data sample of 348 fb^{-1} , which corresponds to $(383 \pm 4) \times 10^6$ $\Upsilon(4S)$ decays into $B\bar{B}$ pairs collected with the *BABAR* detector at the asymmetric-energy e^+e^- PEP-II collider. The *BABAR* detector is described in detail elsewhere [6]. We use the Geant4 simulation toolkit [7] to simulate interactions of particles traversing the *BABAR* detector, and to take into account the varying detector conditions and beam backgrounds.

We fully reconstruct B^0 mesons [8] decaying into a CP eigenstate. From the remaining particles in the event, the vertex of the other B meson, B_{tag} , is reconstructed and its flavor is identified (tagged). The proper decay time difference $\Delta t = t_{CP} - t_{\text{tag}}$, between the signal B (t_{CP}) and B_{tag} (t_{tag}) is determined from the measured distance between the two B decay vertices projected onto the boost axis and the boost ($\beta\gamma = 0.56$) of the center-of-

mass (c.m.) system. The Δt distribution for the signal is given by:

$$F_{\pm}(\Delta t) = \frac{e^{-|\Delta t|/\tau}}{4\tau} [1 \mp \Delta w \pm (1 - 2w)(\eta_f \mathcal{S} \sin(\Delta m \Delta t) - \mathcal{C} \cos(\Delta m \Delta t))], \quad (1)$$

where the upper (lower) sign is for events with B_{tag} being identified as a B^0 (\bar{B}^0), η_f is the CP eigenvalue of the final state, Δm is the B^0 - \bar{B}^0 mixing frequency, τ is the mean lifetime of the neutral B meson, the mistag parameter w is the probability of incorrectly identifying the flavor of B_{tag} , and Δw is the difference of the mistag probability for B^0 and \bar{B}^0 . The tagging algorithm [9] has six mutually exclusive categories and a measured total effective tagging efficiency of $(30.4 \pm 0.3)\%$. The parameters \mathcal{S} and \mathcal{C} describe the amount of CP violation. Neglecting CKM-suppressed decay amplitudes, we expect $\mathcal{S} = -\sin 2\beta$ and $\mathcal{C} = 0$ in the SM. A non-zero value of the parameter \mathcal{C} would indicate direct CP violation.

We reconstruct B^0 mesons using their decays into $D^{(*)0}\pi^0$ ($D^0 \rightarrow K^+K^-$, $K_s^0\omega$) [10] and $D^{(*)0}\eta$ ($D^0 \rightarrow K^+K^-$) with $D^{*0} \rightarrow D^0\pi^0$, and $D^0\omega$ ($D^0 \rightarrow K^+K^-$, $K_s^0\omega$, $K_s^0\pi^0$). The selection criteria are determined by maximizing the expected signal significance based on Monte Carlo (MC) simulation of signal and generic decays of $B\bar{B}$ and $e^+e^- \rightarrow q\bar{q}$ ($q = u, d, s, c$) continuum events. The selection requirements vary by mode due to different signal yields and background levels.

A pair of energy clusters in the electromagnetic calorimeter, that are isolated from any charged tracks and have the expected lateral shower shape for photons, is considered as a π^0 candidate if both cluster energy deposits exceed 30 MeV and the associated invariant mass of the pair is between 100 and 160 MeV/ c^2 . Charged tracks are considered as pions, except for those used in $D^0 \rightarrow K^+K^-$ reconstruction, where the kaons must be consistent with the kaon hypothesis [11]. We reconstruct η mesons in $\gamma\gamma$ and $\pi^+\pi^-\pi^0$ modes. Each photon is required to have an energy exceeding 100 MeV and, when combined with any other photon in the event, to not have an invariant mass within 5 MeV/ c^2 of the π^0 nominal mass [12]. The invariant mass is required to be within approximately 30 MeV/ c^2 (8 MeV/ c^2) of the η nominal mass for $\eta \rightarrow \gamma\gamma$ ($\eta \rightarrow \pi^+\pi^-\pi^0$). Both π^0 and $\eta \rightarrow \gamma\gamma$ candidates are kinematically fitted with their invariant masses constrained at their respective nominal values. The ω mesons are reconstructed from their decays to $\pi^+\pi^-\pi^0$.

They are accepted if the invariant mass is within approximately $22 \text{ MeV}/c^2$ of the nominal value, depending on the D^0 decay mode. The K_s^0 candidate is reconstructed from a pair of oppositely charged tracks whose χ^2 probability of forming a common vertex is greater than 0.1%. The K_s^0 is required to have a measured flight distance from the primary interaction point in the plane transverse to the beam direction of at least two times the measurement error, and an invariant mass within $10 \text{ MeV}/c^2$ of the K_s^0 nominal mass.

The vector meson ω is fully polarized in $D^0 \rightarrow K_s^0 \omega$ decays. Two angular distributions of the ω decay are used to discriminate against background: (a) $\cos \theta_N^D$, defined in the ω rest frame, the cosine of the angle between the D^0 direction and the normal to the decay plane of $\omega \rightarrow \pi^+ \pi^- \pi^0$, and (b) $\cos \theta_D^D$, the cosine of the angle between the direction of one pion in the rest frame of the remaining pion pair and the direction of the pion pair. The signal are distributed according to $\cos^2 \theta_N^D$ and $1 - \cos^2 \theta_D^D$, while the background distributions are nearly uniform. We require $|\cos \theta_N^D| > 0.4$ and $|\cos \theta_D^D| < 0.9$.

For the D^0 in $D^{*0} \rightarrow D^0 \pi^0$, the invariant mass of the D^0 candidate is required to be within $30 \text{ MeV}/c^2$ of the world-average D^0 mass. For the D^0 in $B^0 \rightarrow D^0 h^0$, the invariant mass window is tightened, ranging from ± 14 to $\pm 29 \text{ MeV}/c^2$, depending on the mode. In both cases the D^0 is kinematically fitted with its mass constrained at its nominal value. The invariant mass difference between D^{*0} and D^0 candidates is required to be within $\pm 2.7 \text{ MeV}/c^2$ of the nominal value. For $B^0 \rightarrow D^{*0} \pi^0$ with $D^0 \rightarrow K_s^0 \omega$, we require $|\cos \theta_H^*| > 0.4$, where θ_H^* is the angle between the momenta of the B^0 and the π^0 from the D^{*0} in the D^{*0} rest frame.

We characterize the signal using the kinematic variables $m_{\text{ES}} = \sqrt{(s/2 + \mathbf{p}_0 \cdot \mathbf{p}_B)^2 / E_0^2 - \mathbf{p}_B^2}$, and $\Delta E = E_B^* - E_b^*$, where (E_0, \mathbf{p}_0) is the four-momentum of the e^+e^- system, \mathbf{p}_B is the B^0 momentum, both in the laboratory frame, \sqrt{s} is the c.m. energy, and E_b^* (E_B^*) is the beam (B candidate) energy in the c.m. frame. For signal events, m_{ES} peaks near the B^0 mass with a resolution of about $3 \text{ MeV}/c^2$ and ΔE peaks near zero, indicating that the B^0 candidate has a total energy consistent with the beam energy in the c.m. frame. We require $m_{\text{ES}} > 5.23 \text{ GeV}/c^2$. The ΔE distribution for signal events is asymmetric and varies by decay mode. Depending on the mode, the lower (upper) boundary of the ΔE selection window varies from -95 to -35 MeV ($+35$ to $+85 \text{ MeV}$). The reconstructed $|\Delta t|$ and its uncertainty $\sigma_{\Delta t}$ are required to satisfy $|\Delta t| < 15 \text{ ps}$ and $\sigma_{\Delta t} < 2.5 \text{ ps}$.

The background from continuum $q\bar{q}$ production is suppressed based on the event topology. In the c.m. frame, the B mesons are produced nearly at rest and decay isotropically, while the quarks in the process $e^+e^- \rightarrow q\bar{q}$ are produced with large relative momentum and result in a jet-like topology that is distinct from the more spherical $B\bar{B}$ events. The ratio of the second to zeroth order

Fox-Wolfram moments [14], determined from all clusters in the calorimeter with energy greater than 30 MeV and all charged tracks, must be less than 0.5. The continuum background is further suppressed by a Fisher discriminant \mathcal{F} [15], constructed with the following variables, all evaluated in the c.m. frame: (a) L_2/L_0 where $L_i = \sum_j p_j^* |\cos \theta_j^*|^i$, summed over the remaining particles in the event after removing the daughter particles from the B^0 , p_j^* is the momentum of particle j and θ_j^* is the angle of the momentum with respect to the B^0 thrust axis [16]; (b) $|\cos \theta_T^*|$, where θ_T^* is the angle between the B^0 thrust axis and the thrust axis of the rest of the event; (c) $|\cos^2 \theta_B^*|$, where θ_B^* is the angle between the beam direction and the direction of the B^0 ; (d) total event thrust magnitude; and (e) total event sphericity [17].

For $B^0 \rightarrow D^0 \omega$ decays, we add two angular variables to \mathcal{F} : $\cos \theta_N^B$ and $\cos \theta_D^B$, analogous to $\cos \theta_N^D$ and $\cos \theta_D^D$ in $D^0 \rightarrow K_s^0 \omega$. The signal distributions for the B^0 system are the same as those in the D^0 system. The background distributions are close to $2 - \cos^2 \theta_N^B$ and uniform in $\cos \theta_D^B$. The requirement on \mathcal{F} depends on the background level in each mode, and the signal selection efficiency is 60%–86%, while 72% to 94% of background events are rejected.

Within each reconstructed decay chain, the fraction of events that have more than one candidate ranges from less than 1% to about 10%, depending on the mode. We select one candidate with the most signal-like Fisher discriminant value for each mode.

The signal and background yields are determined by a fit to the m_{ES} distribution using a Gaussian distribution for the signal peak and a threshold function [18] for the combinatorial background. The signal yields are reported in Table I, and the m_{ES} distributions are shown in Fig. 1. We investigate potential backgrounds that might peak in the m_{ES} signal region by studying data in the D^0 mass sideband (outside a window of ± 3 standard deviations of the mass peak) and MC-simulated $e^+e^- \rightarrow B\bar{B}$ events. We estimate that $(0.8 \pm 2.6)\%$ of the CP -even signal yield and $(5.4 \pm 2.2)\%$ of the CP -odd signal yield are background, based on the simulation. Approximately half of the peaking background found in simulation is from $B^- \rightarrow D^0 \rho^- (\rightarrow \pi^0 \pi^-)$ with a low momentum π^- . Other sources include $B^0 \rightarrow \pi^+ \pi^- \pi^0$ and $B^0 \rightarrow D^{(*)0} h^0$, with D^0 decaying to a flavor eigenstate, e.g., $K^- \pi^+$. We find that the peaking background from the D^0 mass sideband data in CP -even modes is consistent with the simulation. For CP -odd modes, we find a larger peaking component in D^0 sideband data than expected from simulation. We estimate that the total peaking background fraction for CP -odd events is $(11 \pm 6)\%$, of which 65% arises from charmless decays with potentially large CP -violating asymmetries. We account for this possibility in the systematic uncertainty.

In order to extract CP violating parameters \mathcal{S} and \mathcal{C} , we fit the m_{ES} and Δt distributions of the selected

TABLE I: Signal yields. Uncertainties are statistical only. The CP parity of the D^0 is indicated in the column of D_{CP} . The combined value is from a simultaneous fit to all modes.

| $\eta_f = +1$ (CP even) | | | $\eta_f = -1$ (CP odd) | | |
|-------------------------------|----------|---------------------|-----------------------------|----------|---------------------|
| Mode | D_{CP} | N_{signal} | Mode | D_{CP} | N_{signal} |
| $D_{K_S^0\omega}^0\pi^0$ | - | 26.2 ± 6.3 | $D_{KK}^0\pi^0$ | + | 104 ± 17 |
| $D_{K_S^0\pi^0\omega}^0$ | - | 40.0 ± 8.0 | $D_{KK}^0\eta\gamma\gamma$ | + | 28.9 ± 6.5 |
| $D_{K_S^0\omega}^0$ | - | 23.2 ± 6.8 | $D_{KK}^0\eta_{3\pi}$ | + | 14.2 ± 4.7 |
| $D_{KK}^{*0}\pi^0$ | + | 23.2 ± 6.3 | $D_{KK}^0\omega$ | + | 51.2 ± 8.5 |
| $D_{KK}^{*0}\eta\gamma\gamma$ | + | 9.8 ± 3.5 | $D_{K_S^0\omega}^{*0}\pi^0$ | - | 5.5 ± 3.3 |
| $D_{KK}^{*0}\eta_{3\pi}$ | + | 6.8 ± 2.9 | | | |
| Combined | | 131 ± 16 | | | 209 ± 23 |
| Total | | | | | 340 ± 32 |

flavor-tagged events using a two-dimensional probability density function (PDF). We define three categories of events: signal, peaking background and combinatorial background. The m_{ES} distribution is described in the previous paragraph. The peaking background is assumed to have the same m_{ES} shape as the signal. The signal decay-rate distribution shown in Eq. 1 accounts for dilution due to an incorrect assignment of the flavor of B_{tag} , and is convolved with a sum of three Gaussian distributions, parameterizing the core, tail and outlier parts of the Δt resolution function [11]. The widths and biases of the core and tail Gaussians are scaled by $\sigma_{\Delta t}$. The outlier Gaussian has a fixed mean (0 ps) and width (8 ps) to account for poorly-reconstructed decay vertices. The mistag parameters and the resolution function are determined from a large data control sample of $B^0 \rightarrow D^{(*)-}h^+$ decays, where h^+ is a π^+ , ρ^+ , or a_1^+ meson. The B^0 lifetime and mixing frequency are taken from [13].

We use an exponential decay to model the Δt PDF of the peaking background. We account for possible CP asymmetries in the systematic uncertainty. The Δt PDF for combinatorial background consists of a term with zero lifetime and an oscillatory term. The former accounts for the continuum contribution. The latter has the same form as the signal PDF; the effective lifetime and the oscillatory coefficients are free parameters in the fit to account for possible CP asymmetry in the background. The sum of a core Gaussian and an outlier Gaussian is sufficient to model the resolution function. The combinatorial background parameters are determined predominantly by the events in the m_{ES} sideband.

A total of 755 events with a well-defined flavor tag are used to fit all decay modes simultaneously. There are 25 free parameters including the m_{ES} shape, the background resolution function, the CP parameters of signal and background, and the fractions of the combinatorial background. We obtain $\mathcal{S} = -0.56 \pm 0.23 \pm 0.05$ and $\mathcal{C} = -0.23 \pm 0.16 \pm 0.04$, where the first errors are statistical and the second are systematic. The statistical

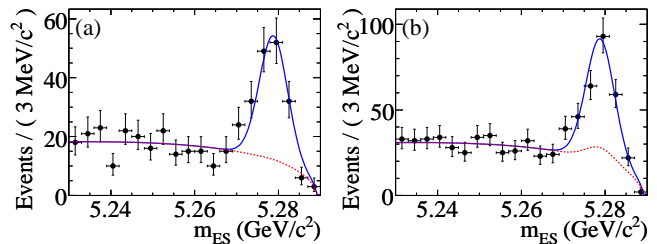


FIG. 1: The m_{ES} distributions with a fit to (a) the CP -even and (b) the CP -odd modes combined in the data. The solid curve represents the overall PDF projection and the dashed curve represents the background.

correlation between \mathcal{S} and \mathcal{C} is $\rho(\mathcal{S}, \mathcal{C}) = -2.4\%$. The Δt distribution projections and the asymmetry ($A = [N_{B^0\text{tag}}(\Delta t) - N_{\bar{B}^0\text{tag}}(\Delta t)]/[N_{B^0\text{tag}}(\Delta t) + N_{\bar{B}^0\text{tag}}(\Delta t)]$) for the events in the signal region are shown in Fig. 2. We check the consistency between CP -even and CP -odd modes by fitting them separately and find (errors are statistical only) $\mathcal{S}_{\text{even}} = -0.17 \pm 0.37$, $\mathcal{S}_{\text{odd}} = -0.82 \pm 0.28$, and $\mathcal{C}_{\text{even}} = -0.21 \pm 0.25$, $\mathcal{C}_{\text{odd}} = -0.21 \pm 0.21$. The difference between $\mathcal{S}_{\text{even}}$ and \mathcal{S}_{odd} is 0.65 ± 0.46 , less than 1.5 standard deviation from the expected value, zero. We also find that the differences between $h^0 \rightarrow \gamma\gamma$ and $h^0 \rightarrow \pi\pi\pi$ modes are less than 0.1 in \mathcal{C} and \mathcal{S} .

The SM corrections due to the sub-leading-order diagrams are different for D_{CP+} and D_{CP-} [4]. Therefore, we also perform a fit allowing different CP asymmetries for D_{CP+} and D_{CP-} . We obtain $\mathcal{S}_+ = -0.65 \pm 0.26 \pm 0.06$, $\mathcal{C}_+ = -0.33 \pm 0.19 \pm 0.04$, $\rho(\mathcal{S}_+, \mathcal{C}_+) = 4.5\%$, and $\mathcal{S}_- = -0.46 \pm 0.45 \pm 0.13$, $\mathcal{C}_- = -0.03 \pm 0.28 \pm 0.07$, $\rho(\mathcal{S}_-, \mathcal{C}_-) = -14\%$.

The dominant systematic uncertainties are from the peaking background and the m_{ES} peak shape uncertainties (0.04 in \mathcal{S} and 0.03 in \mathcal{C}). For the former, we vary the amount of the peaking background according to its estimated uncertainty, and vary the CP asymmetry of the charmless component between $\pm \sin 2\beta$ of the world-average value. We study the latter effect using an alternative line shape [19] taking into account a possible non-gaussian tail in the m_{ES} distribution. It would be possible to reduce these uncertainties with a larger data sample in the future. Other systematic uncertainties, studied by varying the fit configuration and fixed parameters, are listed below in order of importance (typically not exceeding 0.01 in \mathcal{S} and \mathcal{C}). The signal Δt resolution function and mistag parameters are varied according to the uncertainties in the data control sample. The difference in the resolution function in MC samples between the signal modes and the modes used in the data control sample is also considered a source of uncertainty. The width of the m_{ES} distribution for the peaking background is varied to account for possible difference between the signal and the peaking background. The end

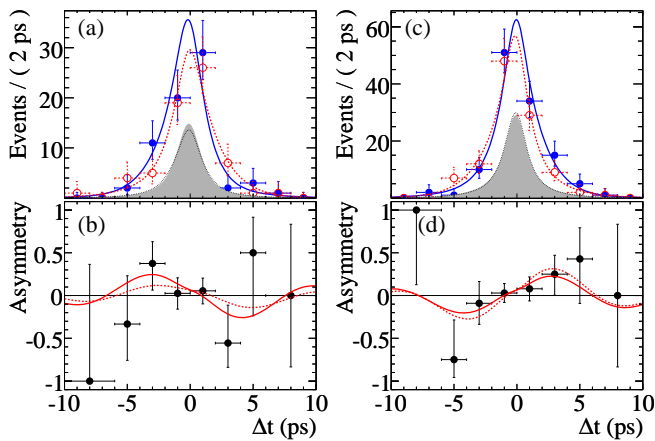


FIG. 2: The Δt distributions and asymmetries for (a,b) CP -even and (c,d) CP -odd events in the signal region ($m_{ES} > 5.27 \text{ GeV}/c^2$). In (a) and (c), the solid points with error bars and solid curve (open circles with error bars and dashed curve) are B^0 -tagged (\bar{B}^0 -tagged) data points and Δt projection curves. Shaded areas (B^0 -tagged) and the dotted lines (\bar{B}^0 -tagged) are background distributions. In (b) and (d), the solid curve represents the combined fit result, and the dashed curve represents the result of the fits to CP -even and CP -odd modes separately.

point of the m_{ES} threshold function is varied to account for the variation of the beam energy. The interference between the CKM-suppressed $\bar{b} \rightarrow \bar{u}c\bar{d}$ and CKM-favored $b \rightarrow \bar{c}u\bar{d}$ amplitudes in the final states used for B -flavor tagging gives deviations from the standard time evolution function Eq. 1 [20]. This effect is studied with simulation. Lifetime and mixing are varied over their uncertainties [13]. The beam-spot position and size in the vertical direction are varied by $20 \mu\text{m}$. Uncertainties due to the vertex tracker length scale and alignment are negligible. Summing over all systematic uncertainties in quadrature, we obtain 0.05 for \mathcal{S} and 0.04 for \mathcal{C} .

In conclusion, we have measured the time-dependent CP asymmetry parameters $\mathcal{S} = -0.56 \pm 0.23 \pm 0.05$ and $\mathcal{C} = -0.23 \pm 0.16 \pm 0.04$ from a sample of 340 ± 32 $B^0 \rightarrow D_{CP}^{(*)}h^0$ signal events. The result for \mathcal{S} is consistent with the world average $-\sin 2\beta = -0.725 \pm 0.037$ [13], and is 2.3 standard deviations from the CP -conserving hypothesis $\mathcal{S} = \mathcal{C} = 0$.

We are grateful for the excellent luminosity and machine conditions provided by our PEP-II colleagues, and for the substantial dedicated effort from the computing organizations that support BABAR. The collaborating institutions wish to thank SLAC for its support and kind hospitality. This work is supported by DOE and NSF (USA), NSERC (Canada), IHEP (China), CEA and

CNRS-IN2P3 (France), BMBF and DFG (Germany), INFN (Italy), FOM (The Netherlands), NFR (Norway), MIST (Russia), MEC (Spain), and PPARC (United Kingdom). Individuals have received support from the Marie Curie EIF (European Union) and the A. P. Sloan Foundation.

* Deceased

† Also with Università di Perugia, Dipartimento di Fisica, Perugia, Italy

‡ Also with Università della Basilicata, Potenza, Italy

§ Also with IPPP, Physics Department, Durham University, Durham DH1 3LE, United Kingdom

- [1] B. Aubert *et al.* (BABAR Collaboration) Phys. Rev. Lett. **94**, 161803 (2005); K.-F. Chen *et al.* (Belle Collaboration), Phys. Rev. Lett. **98**, 031802 (2007).
- [2] N. Cabibbo, Phys. Rev. Lett. **10**, 531 (1963); M. Kobayashi and T. Maskawa, Prog. Theoret. Phys. **49**, 652 (1973).
- [3] Y. Grossman and M. P. Worah, Phys. Lett. B **395**, 241 (1997).
- [4] R. Fleischer, Phys. Lett. B **562**, 234 (2003); R. Fleischer, Nucl. Phys. B **659**, 321 (2003).
- [5] See, for example, the review of CP violation in meson decays in [13] and the references therein.
- [6] B. Aubert *et al.* (BABAR Collaboration), Nucl. Instrum. Meth. A **479**, 1 (2002).
- [7] S. Agostinelli *et al.* (Geant4 Collaboration), Nucl. Instrum. Meth. A **506**, 250 (2003).
- [8] Unless explicitly stated, charge conjugate reactions are implicitly included throughout the paper.
- [9] B. Aubert *et al.* (BABAR Collaboration), Phys. Rev. Lett. **94**, 161803 (2005).
- [10] All neutral D mesons in this Letter decay to CP eigenstates. Therefore the notation $D^{(*)0}$ implies $D_{CP}^{(*)0}$.
- [11] B. Aubert *et al.* (BABAR Collaboration), Phys. Rev. D **66**, 032003 (2002).
- [12] All nominal masses are from [13].
- [13] W.-M. Yao *et al.* (Particle Data Group), J. Phys. G **33**, 1 (2006).
- [14] G. C. Fox and S. Wolfram, Phys. Rev. Lett. **41**, 1581 (1978).
- [15] R. A. Fisher, Annals of Eugenics **7**, 179 (1936).
- [16] S. Brandt *et al.*, Phys. Lett. **12**, 57 (1964); E. Fahri, Phys. Rev. Lett. **39**, 1587 (1977).
- [17] J. D. Bjorken and S. J. Brodsky, Phys. Rev. D **1**, 1416 (1970).
- [18] H. Albrecht *et al.* (ARGUS Collaboration), Phys. Lett. B **241**, 278 (1990).
- [19] M. J. Oreglia, Ph.D. Thesis, SLAC-236 (1980), Appendix D; J. E. Gaiser, Ph.D. Thesis, SLAC-255 (1982), Appendix F; T. Skwarnicki, Ph.D. Thesis, DESY F31-86-02 (1986), Appendix E.
- [20] O. Long *et al.*, Phys. Rev. D **68**, 034010 (2003).